Journal of Mining and Environment (JME) Vol. 16, No. 1, 2025, 241-258

Shahrood University of Technology

Journal of Mining and Environment (JME)

Journal homepage: www.jme.shahroodut.ac.ir

Iranian Society of Mining Engineering (IRSME)

Simulating the Hydraulic Fracturing Mechanism Around the Hydrocarbon Wellbores with Emphasizing its Effects on the Sand Production

Masoud Yazdani, Mohammad Fatehi Marji*, Mehdi Najafi, and Manouchehr Sanei

Department of Mining and Metallurgical Engineering, Yazd University, Yazd, Iran

Article Info

Received 10 January 2024

Received in Revised form 10 January 2024

Accepted 13 May 2024

Published online 13 May 2024

DOI: 10.22044/jme.2024.14049.2619

Keywords

Discrete element method

Hydraulic fracturing

Sand production

Oil well

Abstract

Around 70% of the world's hydrocarbon fields are situated in reservoirs containing low-strength rocks, such as sandstone. During the production of hydrocarbons from sandstone reservoirs, sand-sized particles may become dislodged from the formation and enter the hydrocarbon fluid flow. Sand production is a significant issue in the oil industry due to its potential to cause erosion of pipes and valves. Separating grains from oil is a costly process. Oil and gas companies are motivated to reduce sand production during petroleum extraction. Hydraulic fracturing is one of the parameters that can influence sand production. However, understanding the complex interactions between hydraulic fracturing mechanisms and sand production around wellbores is critical for optimizing reservoir recovery and ensuring the integrity of production wells. This article explores the integrated simulation approach to model hydraulic fracturing processes and assess their effects on sand production. Two-dimensional models were created using the discrete element method in PFC2D software for this research. The fractures' length in the models varies based on the well's radius. The angle between two fractures at 90 and 180 degrees to each other was also modeled. In the first case, the length of the fracture is less than the radius of the well, in the second case, the values are equal and finally, the fracture length is assumed to exceed the well radius. The calibrated and validated results demonstrate the change in sand production rate in comparison to the unbroken state.

1. Introduction

As a technique for fracturing underground rock formations using pressurized fluid, hydraulic fracturing has been used extensively in areas as diverse as reservoir stimulation, in-situ stress estimation, caving and fracture response in mining, geothermal energy extraction, and subsurface environmental remediation [1, 2, and 3]. Hydraulic fracturing is a crucial technique for extracting oil and gas from unconventional reservoirs. It creates fracture networks that serve as transport paths in tight formations. Since the first field test was performed on a gas well at the Hugoton field in 1947 [4], hydraulic fracturing has been extensively researched by both academia and industries using experimental tests, field trials, and numerical simulations [5, 6]. In order to facilitate the study of hydraulic fracturing, certain aspects of the problem must be simplified or disregarded in analytical and numerical investigations. This has resulted in the development of various modelling approaches with different levels of applicability and limitations. Hydraulic fracturing modelling has been extensively studied by researchers in both petroleum engineering and fracture mechanics [7, 8, and 9]. Numerous hydraulic fracturing models have been developed to improve the design of hydraulic fracturing treatments or to understand some specific mechanisms such as screen-out, near-wellbore tortuosity, etc. During the period

✉ *Corresponding author: mohammad.fatehi@gmail.com (M. Fatehi Marji)*

from the 1950s to the 1980s, several classic hydraulic fracturing models were developed [10]. These include the Kristianovich-Geertsma-de Klerk (KGD) model, the Perkins-Kern-Nordgren (PKN) model, the pseudo 3D (P3D) model, and the planar 3D (PL3D) model. The P3D and PL3D models have remained popular in commercial simulators for hydraulic fracturing design until recently. However, in recent decades, a wider range of numerical methods, such as the finite element method (FEM), the extended finite element method (XFEM), and the discrete element method (DEM), have been applied and adapted to model hydraulic fracturing [11]. Eshiet et al. [12] simulated hydraulic fracturing in materials with mechanical properties resembling rock and soil. The study investigates the effects of injection parameters and rock properties on hydraulic fracture initiation and propagation using PFC2D [13]. Hofmann et al. [14] simulated the simultaneous propagation of multiple hydraulic fractures under different completion designs (stage spacing, wellbore spacing, etc.) and treatment parameters. The fracture patterns obtained in these numerical cases were transferred to a finite element reservoir model to investigate the impact of completion design and treatment parameters on the efficiency of fracture networks. Shimizu et al. [15] investigated the influence of heterogeneous particle size and fluid viscosity on initiation and propagation of hydraulic fractures using a DEM code. The indirect boundary element method in form of the modified displacement discontinuity method is also used for the simulation of hydraulic fracturing mechanism in porous and fractured rocks [16-19].

Hydraulic fracturing operations can be a contributing factor to sand production. Sand production is a common occurrence in oil wells. In order to develop an optimal well completion and recovery strategy, predicting sand production and its rate is critical. Various methods, including analytical, experimental, and numerical, are used to predict sand production. These methods are highly complementary. They should be combined to ensure a realistic and consistent approach to sand production prediction. According to sources [20, 21], this phenomenon is common. Field observations indicate that perturbations in flow gradients and effective stress acting on the porous matrix of the formation initiate the fracturing of small portions of the rock. According to the Society of Petroleum Engineers (SPE), a significant portion of the world's hydrocarbon reserves are contained in sandstone and are therefore susceptible to this phenomenon. According to research [22], approximately seventy percent of the world's hydrocarbon reserves are found in reservoirs where sand/solids production may occur. Bianca [22] proposed that the production of sand/solids in oil-producing wells is influenced by three main factors: the magnitude and variation of in-situ stresses, pressure gradients, fluid flow velocity, changes in fluid saturation, the strength factor (material strength, inter-particle friction, sand arches, and capillary forces), and operational factors (drilling and completion strategies, production procedures, and reservoir depletion). For more information on sand/solids production operational aspects and mechanisms, refer to [20, 22]. Previous studies have highlighted the difficulty in predicting sand production [15, 20]. Furthermore, the numerical modelling of this phenomenon is complex due to the intricate interaction between fluid and solid [24, 25, and 26].

The article [27] provides a detailed description of the tests and modeling of sand production. The present research results are compared with those of previous studies. This research examines the impact of fractures on sand production in models. The software PFC2D-generated model represents a laboratory-scale, two-dimensional cross-section of an oil well. The length of the fracture changes according to the radius of the well. In the first three cases, the length of the fracture is shorter than the radius of the well (a=15 mm, r = 30 mm). The next state is when the radius is equal to the fracture length (a=30 mm, r = 30 mm). In the last three cases, the length of the modeled fracture is considered to be greater than the radius (a=50 mm, r = 30 mm).When fractures are added to the model, the amount of sand production is measured.

2. Physical Processes and Mathematical Models

Hydraulic fracturing is a process used to fracture underground rocks by injecting pressurised fluid into the formation, as shown in Figure 1. The process involves three basic steps: (1) deformation of rocks around the fracture; (2) fluid flow in the fracture; and (3) fracture initiation and propagation [3, 28]. Hydraulic fracturing involves not only basic physical processes but also several secondary physical phenomena. These secondary processes are often considered in various analytical and numerical models.

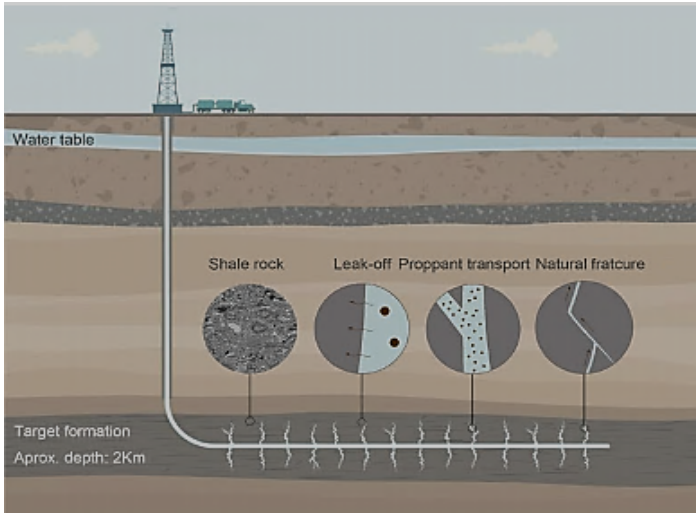

Figure 1. Hydraulic fracturing as a multistage and multi-physics process [28].

2.1. Rock Deformation

Rock deformation is determined by rock properties and related boundary conditions, such as fluid pressure and in-situ stresses. The heterogeneous nature of rock formations makes it difficult to represent realistic rock properties in a numerical model. Additionally, rock deformation often exhibits Elastoplastic behaviour, which is further complicated by its porosity. Linear elasticity is one of the most widely adopted simplifications. The equilibrium condition of rocks is expressed as:

$$\nabla\sigma + \rho g = \rho u \quad (1)$$

Where ρ denotes the local density of rock, g the gravity acceleration, and u the displacement. In certain cases, such as a linear fracture in two-dimensional space or a planar fracture in three-dimensional space, the width of the fracture can be directly calculated using analytical solutions derived from elasticity theory [29, 30, and 31]. Poroelasticity has been widely adopted to consider the effect of porosity and pore pressure in rock formation. According to Biot's consolidation theory [32], additional parameters are introduced to describe rock properties, such as the Biot modulus, effective stress coefficient, rock permeability, and existing pore pressure. Rock deformation is calculated and presented differently depending on the numerical discretization approach used. In continuum-based methods, such as the boundary element method and FEM, deformation is calculated based on a discretization mesh and presented by nodal values. In discontinuum-based methods, deformation is calculated and presented by the movement of particles or blocks. The method used to calculate rock deformation has an impact on other numerical components in a hydraulic fracturing model. This is a crucial aspect of hydraulic fracturing simulators.

2.2. Fluid Flow in the Rock Fracture

Hydraulic fracturing differs from traditional fragmentation problems due to the intrinsic coupling between fracture propagation and fluid flow, making it more challenging to model. To consider the effect of fluid flow in the numerical framework of hydraulic fracturing, a uniform fluid pressure can be applied to the fracture surface [33]. However, this simplified approach can cause significant modelling errors, except for certain special cases with low viscosity fluids and high toughness formations. A more rational approach to modelling fluid flow in fractures is based on the lubrication theory. This theory recognizes that the aperture of a hydraulic fracture is always much smaller than its height and length [34, 35]. The use of lubrication theory in hydraulic fracturing modelling is widespread, with Poiseuille's law (or cubic law) being commonly employed to relate flow rate to pressure gradient along the hydraulic fracture. In the case of fluid flow in a two-dimensional hydraulic fracture, Poiseuille's law is expressed as:

$$q = \frac{w^3}{12\mu}\frac{dp}{ds} \quad (2)$$

Where q is the flow rate, w is the fracture width, μ is the viscosity of the fracturing fluid, p is the fluid pressure, and s is the local coordinate aligned with the tangential direction to the

fracture path. Taking into account the leakoff effect, the continuity equation is expressed as (where q_l is the leakoff flow rate):

$$\frac{dw}{dt} + \frac{dq}{ds} + q_l = 0 \quad (3)$$

The Poiseuille's law and the continuity equation mentioned above are commonly used in 2D discrete fracture analysis and can be extended to 3D analysis by considering the flow rate and pressure gradient in different directions [36, 37]. The lubrication theory is commonly used to model the pressure drop along the hydraulic fracture due to its ease of implementation and computational efficiency. It is important to note that Poiseuille's law, which is only valid for laminar flow, is the main flow regime during hydraulic fracturing operations. However, turbulent flow may also occur during hydraulic fracturing when the injection flow rate and properties of the fracturing fluid vary over a large range [38, 39].

2.3. Fracture propagation mechanisms

Fracture criterion is an essential component of hydraulic fracture models as it determines fracture propagation. The choice of fracture criterion in hydraulic fracturing simulations largely depends on the specific numerical scheme used to discretise the rock formation. Linear elastic fracture mechanics (LEFM) and cohesive zone models are commonly employed in discrete fracture approaches [40]. The LEFM criteria comprise the maximum tensile stress criterion, the minimum strain energy density criterion, the maximum principal strain criterion, and the maximum strain energy release criterion [41]. Among these, the maximum tensile stress criterion is the most commonly used and can be expressed as:

$$\cos\frac{\theta}{2}\left(k_I \cos\frac{\theta}{2} - \frac{3}{2}k_{II}\sin\theta\right) > k_{Ic} \quad (4)$$

Where k_I, k_{II} and k_{Ic} are the stress intensity factors for the mode I fracture, the mode II fracture and the fracture toughness respectively, and the propagation direction θ is determined by (sgn, denotes the sign function):

$$\tan\frac{\theta}{2} = \frac{1}{4}\left(\frac{k_I}{k_{II}} - sgn(k_{II})\sqrt{\left(\frac{k_I}{k_{II}}\right)^2 + 8}\right) \quad (5)$$

$$-\pi < \theta < \pi$$

The stress intensity factor criteria are typically used when treating rock as a linear elastic material. To account for non-linear mechanical effects, the cohesive zone model, first developed by Dugdale [42] and Barenblatt [43], is commonly used, as shown in Figure 2. This model assumes a process zone ahead of the actual fracture to avoid the singularity near the crack tip. In the process zone, a traction-separation law is introduced to define the relationship between fracture width and cohesive traction. This relationship can take different forms. When simulating fracture propagation using smeared fracture models, the strain threshold and Mohr-Coulomb failure criterion are typically used to determine whether an element will become damaged [44]. For discontinuum based methods, the fracture is represented by the breakage of bonds between particles or blocks, and therefore the corresponding fracture criterion is implicitly determined by the rule of bonds breakage.

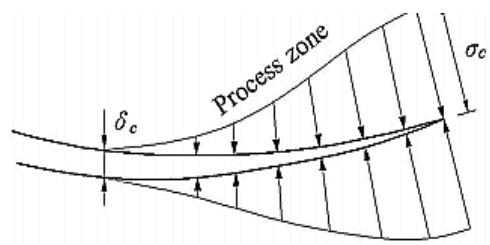

Figure 2. Schematics of zone model, definitions of model parameter [44].

3. Sand Production Mechanisms

Sand production is a process that involves two mechanisms: mechanical instabilities that cause localized plastic behavior and failure of the rock around the cavity, and the subsequent transportation of sand particles due to fluid drag forces. This process is a coupled fluid and solid process [45]. The sandstone rock initially fails close to the cavity, and the failed material is then eroded by the flowing fluid. These two mechanisms are interdependent. Stress concentrations around the eroded cavity result in increased damage, which increases the amount of cohesionless material that can be dislodged. The classical approach focuses on identifying the conditions that trigger sand production, including several failure modes, relevant conditions, and controlling operational variables [46]. Figure 3 illustrates the three-step process of sand production: near-wellbore damage, perforation, and transportation. Sand production initiates with the formation of small holes around the borehole,

which then extend and eventually connect to form a larger hole. This sudden increase in the size of hole causes sand to enter the well [46]. It is important to note that this classification is based on the amount of sand produced in the well over time. To prevent sand production it is necessary to identify and address the underlying causes. Sand production in wells can be caused by a number of factors, including disturbed stratigraphic stress balance, fluid movement, and reduction in reservoir pressure, reduction in structure toughness, rock fatigue and increased production. Sand production is typically classified into three states: unstable, stable and catastrophic [46].

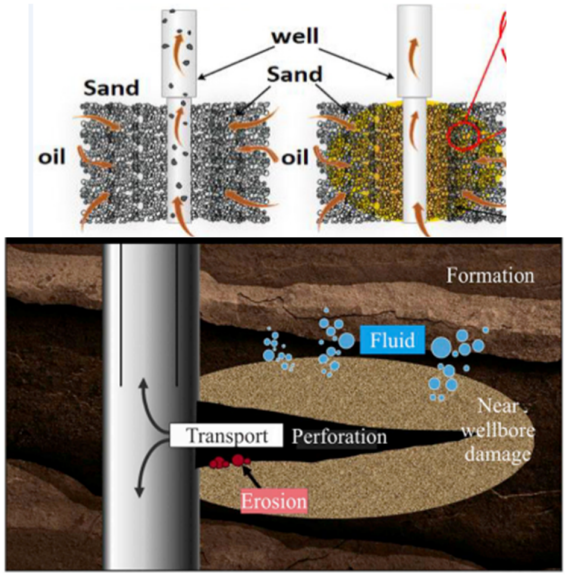

Figure 3. Sand Production Mechanism [46].

4. Discontinuum-Based Methods for Modeling the Hydraulic Fracturing

Cundall [47] was the first to develop a Discrete Element Method (DEM) model for analyzing rock mechanics problems. Unlike the continuum approach, this model describes the rock media as a discrete system of deformable polygonal blocks. The solution procedure alternates between applying Newton's second law for blocks and force-displacement law for contacts between blocks. ITASCA Consulting Group developed a 2D numerical software called Universal Distinct Element Code (UDEC) and its 3D version, Three-Dimensional Distinct Element Code (3DEC), based on this pioneering work. The Particle Flow Code in 2D and 3D (PFC2D and PFC3D) has been developed using DEM, which employs rigid disks or spherical particles in a simplified manner. PFC differs from UDEC and 3DEC in several aspects. Firstly, the discrete elements (disks in 2D and spheres in 3D) are rigid, while the blocks in UDEC or 3DEC can be either deformable or rigid. Secondly, interaction between discrete elements is easier to model in PFC compared with UDEC and 3DEC, making PFC more efficient. Finally, the extent of displacement is not limited in PFC [48]. Fractures in PFC are represented by voids and channels. The interaction between particles can be described by several built-in contact models, which simulate shear and/or tensile forces between particles. Fluid flow is simulated using a void-channel system. The fluid flows through the channel according to Poiseuille's law, while the fluid pressure change inside voids is computed based on the continuity equation and fluid compressibility property [49, 50]. Unlike continuum methods, DEM simulates hydraulic fracturing from a microscopic perspective. The advantages are manifold: (1) no additional fracture criterion is required to control fracture propagation; (2) initiation and propagation of hydraulic fractures can be simulated in a unified framework; and (3) there is no need to update the topology with the propagation of hydraulic fractures. However, the relevant parameters must be calibrated prior to application to ensure accurate modelling of the macro scale mechanical behaviour of the rock [51].

4.1. Research Methodology

When modelling particles and materials, the most appropriate method is the discrete element method, and it is recommended to use PFC software. Modelling any type of test using PFC2D software involves two main coding parts. The first part consists of creating a sample with appropriate specifications, such as compression, porosity, and desired geometry, with standard dimensions. The second part involves uploading the sample. The standard process for creating samples for rock modelling includes five steps:

i) The initial step is to compress the granular particles by creating walls using flat and frictionless plates. Then, a set of particles with the desired distribution is produced to fill the container. The number of particles used in the initial compaction is determined to achieve the desired initial porosity of the model in the particle assembly container. The particles are placed randomly in the environment with a maximum radius equal to half the desired radius to prevent overlap. Then, the particle radius is increased to

achieve the desired porosity for the modeled assembly.

ii) To achieve isotropic stress in the particle assembly, the radius of all particles within the container is reduced. The isotropic stress condition is obtained by calculating the average direct stress, which is the result of dividing the total force on the walls by the cross section of the modeled sample.

iii) To create a reliable geometrical model, it is advisable to exclude or limit the amount of suspended (unattached) particles in the particle assembly.

iv) To create appropriate parallel bonds between particles in the assembly, a regular network is formed in all adjacent particles. This is achieved when the distance between surfaces is less than 10 times the average radius of the two particles.

v) The production process entails eliminating floating particles and walls from the model's periphery, enabling it to move freely and reach equilibrium.

Before conducting numerical modelling and verifying the mechanism, it is essential to create an artificial rock sample and calibrate the numerical model using the laboratory artificial rock. This ensures that the macromechanical behaviour of the numerical model of the artificial rock, such as uniaxial, triaxial, and Brazilian resistance, aligns with the mechanical behaviour of the virgin rock. The modelling is performed in two dimensions using the Particle Flow Code (PFC2D). Calibration was carried out using laboratory test results for the uniaxial compressive strength of two artificial sandstone rocks.

4.2. Model geometry

This section outlines the simulation of a synthetic sanding test using the DEM model. The model geometry and boundary conditions are specified first, followed by a description of the results of a series of sensitivity analyses to optimize. The DEM model was created in a rectangular box with a length and width of 150 mm each. The domain is bounded by four frictionless rigid walls, as shown in Figure 6. Parallel bonds were randomly imposed on 30% of the contacts after the material generation stage. The bond radius multiplier was randomly varied between 0 and 1, as described by Rahmati (2013) [52]. The vertical borehole with 30 mm radius was drilled by gradually decreasing the grain stiffness inside the borehole to zero followed by removing the grains inside the borehole. Initial analysis was carried out until the average unbalanced forces divided by the average contact forces was smaller than 1%. The fluid flow model was linked to the DEM model.

The article [27] provides a detailed description of the tests and modeling of sand production. The present research results are compared with those of previous studies. This research examines the impact of fractures on sand production in models. Fractures in the form of Figure 4 are added to the models, and the amount of sand production is measured.

In all cases, the stress value is equal to 35 MPa and the fluid pressure is equal to 2 MPa [27]. In the first three cases, the length of the fracture is shorter than the radius of the well. We also check to include a fracture angled different from the first (a=15 mm, r = 30 mm). The next state is when the radius is equal to the fracture length (a=30 mm, r = 30 mm). In the last three cases, the length of the modeled fracture is considered to be greater than the radius (a=50 mm, r = 30 mm), Figure 5.

4.3. Calibration of the geomaterial model

Numerical modelling using FLAC and UDEC software requires the direct extraction of macro-mechanical properties such as Young's modulus, Poisson's ratio and uniaxial resistance from laboratory results and their application to the model. In PFC, it is not possible to directly apply macromechanical properties to the model. Instead, the ideal macromechanical properties of the model should be estimated by selecting appropriate micromechanical properties, such as normal and shear stiffness of connections and Young's modulus of connections. This will ensure that the numerical and laboratory macromechanical behavior is similar. The two samples chosen for calibration are from Natalia Pera's work (Natalia Pera, 2016) [54]. The single-axis machine contains the same two samples, 1 and 2, used in the laboratory stage [27]. Table 1 provides the specifications and features of these samples. The particles are disk-shaped, with a diameter ratio greater than 1 between the largest and smallest grains. If the grain dimensions are equal (ratio = 1), the behavior will be isotropic, which differs from the natural behavior of rock grains. For this analysis, dimensions of 0.6 and 0.7 were selected to reflect static conditions.

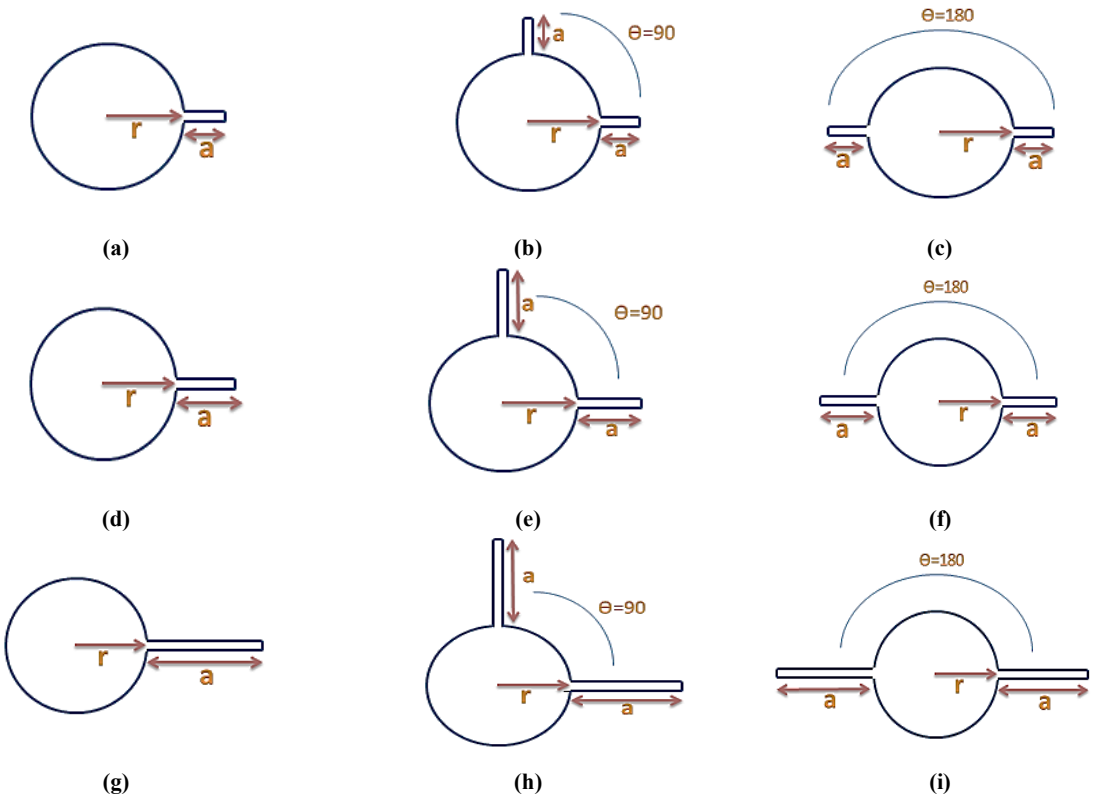

Figure 4. The fractures created in the modeling around the well with a radius of 30 mm, a) One fracture (a< r), b) Two fractures with an angle of 90 degrees to each other (a< r), c) Two fractures with an angle of 180 degrees to each other (a< r), d) fracture (a= r), e) Two fractures with an angle of 90 degrees to each other (a= r), f) Two fractures with an angle of 180 degrees to each other (a= r), g) fracture (a> r), h) Two fractures with an angle of 90 degrees to each other (a>r), i) Two fractures with an angle of 180 degrees to each other (a> r).

Table 1. Micro-Parameters for calibration

Micro parameters	Sample 1	Sample 2
Particle type	Disc	Disc
Density (g/cm3)	1.92	1.74
Minimum disk radius	0.2	0.2
damping coefficient	0.7	0.6
Young's modulus of contact (GPa)	15	13.8
Hardness ratio of contact connection	3.6	2.9
Young's modulus of parallel connection (GPa)	15	13.8
Parallel connection stiffness ratio	3.6	2.9
friction coefficient	0.4	0.4
Normal resistance of parallel connection (MPa)	29	31.5
Shear strength of parallel connection (MPa)	29	31.5
Parallel bond adhesion (MPa)	14.5	15

For the uniaxial compression test simulation, we used a model depicted in Figure 6. The model has a height of 110 mm and a width of 50 mm, and both samples have the same dimensions. The loading is simulated by two moving plates that apply pressure to the set of disks.

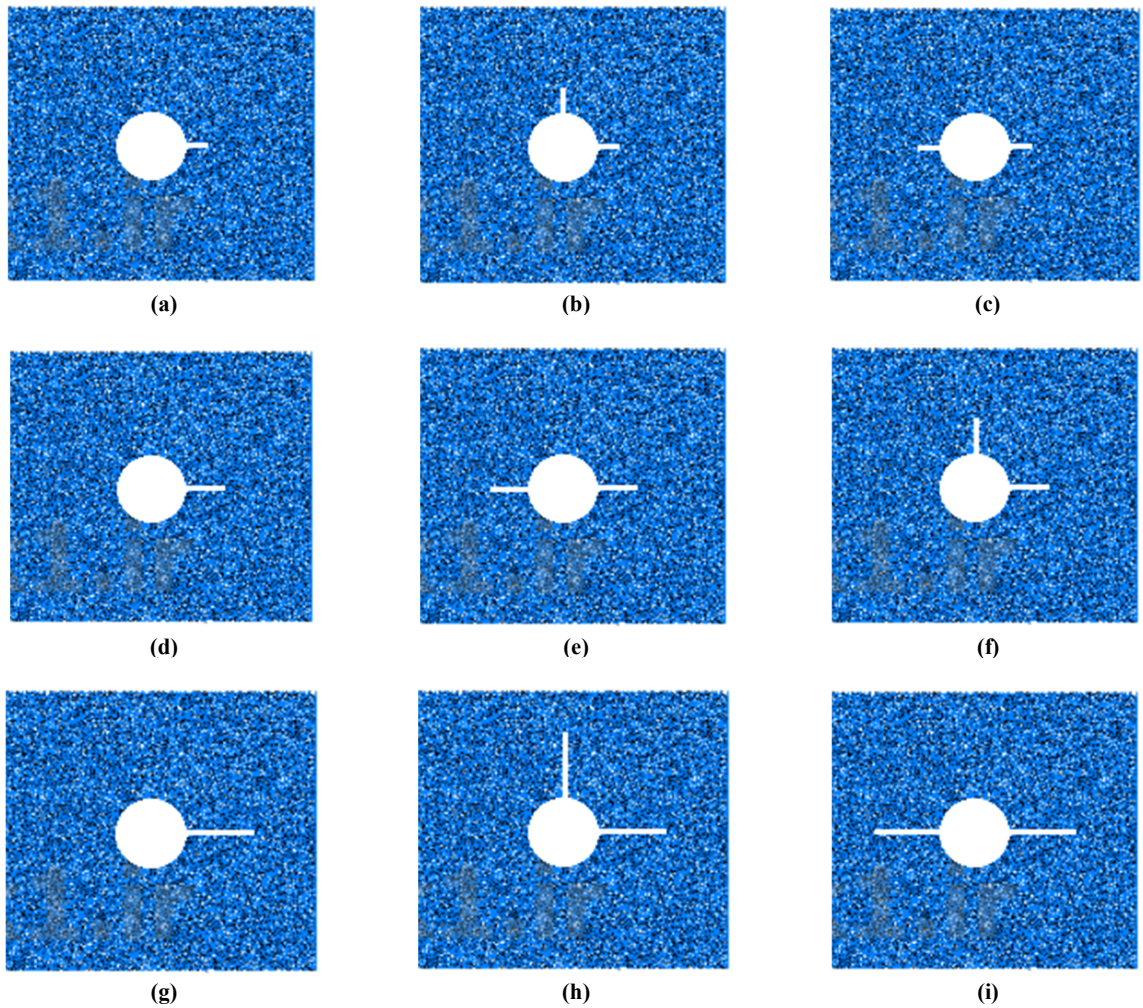

Figure 5. Models made in the PFC2D by creating different fractures, a) One fracture (a< r), b) Two fractures with an angle of 90 degrees to each other (a< r), c) Two fractures with an angle of 180 degrees to each other (a< r), d) fracture (a= r), e) Two fractures with an angle of 90 degrees to each other (a= r), f) Two fractures with an angle of 180 degrees to each other (a= r), g) fracture (a> r), h) Two fractures with an angle of 90 degrees to each other (a>r), i)) Two fractures with an angle of 180 degrees to each other (a> r).

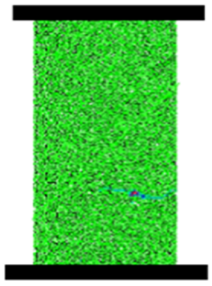

Figure 6. Model built under uniaxial test, height of 110 mm and a width of 50 mm.

Figure 7(a) shows the stress-strain diagram obtained from the numerical simulation of sandstone 1 and the fracture pattern of the numerical model. In (b), the stress-strain diagram obtained from the numerical simulation for sample 2 is displayed. The results of the uniaxial compressive strength test in this research are in acceptable agreement with the numerical and laboratory results of two sandstone samples, as presented in Table 2. This table will be used for further discussions and modelling in the software.

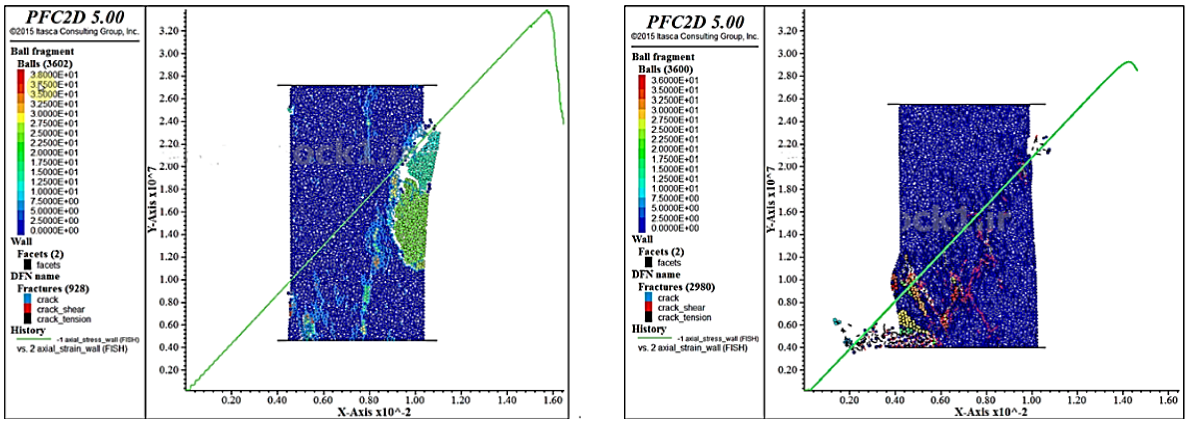

(a) (b)

Figure 7. Stress-strain diagram obtained from numerical modeling of: a) sample 1, b) sample 2.

Table 2. Macromechanical parameters for calibration in PFC2D

Young's modulus (Gpa)	Poisson's ratio	Uniaxial compressive strength (MPa)	The results of the samples as:	
8.5	-	33	Laboratory	Sample 1
8.5	0.18	31.8	(Natalia pera, 2016)	
7	0.15	36	Numerical modeling of this article	
6	-	28	(Natalia pera, 2016)	Sample 2
6.5	0.19	26.5	Numerical modeling in this research	
4.5	0.15	32		

4.4. Validation

To ensure objectivity, the numerical modelling results obtained from PFC2D should be validated by model fitting with the laboratory test results. In this study, we compare the fluid pressure parameters with the laboratory results of Natalia in 2016 (Natalia Pera, 2016) [54] and the simulation results of [53]. We use the calibration results of Sandstone B for validation. To simulate sand production, we constructed a sample measuring 15x15 cm with a 3 cm diameter hole containing disc particles ranging from 0.2 to 0.3 mm in radius, using the data from [27]. Figure 8 illustrates the constructed example.

Figure 9(a) displays the simulation results in PFC2D software, while (b) shows the Yifie results from 2016 [53] for the case where the fluid pressure is 10 MPa. The way in which the particles are separated and emptied around the wall is in good agreement with the 2016 Yifie results. Figure 9(c) presents the simulation results in PFC2D software, and (d) shows the Yifie results from 2016 [53] for the case where the fluid pressure is 25 MPa. The results of the uniaxial test modelling in this study are in relatively good agreement with the uniaxial compressive strength results of Sandstone B, with a difference of approximately 10%. Additionally, the simulation results from both PFC2D software and Yifie in 2016 demonstrate that PFC2D software is a reliable and accurate tool for modelling sand production mechanisms.

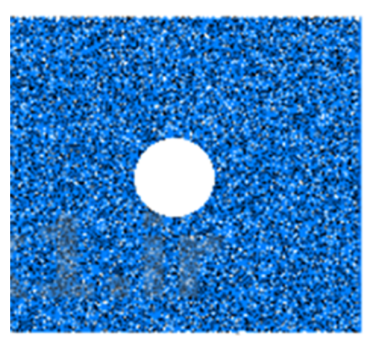

Figure 8. Model made in PFC2d.

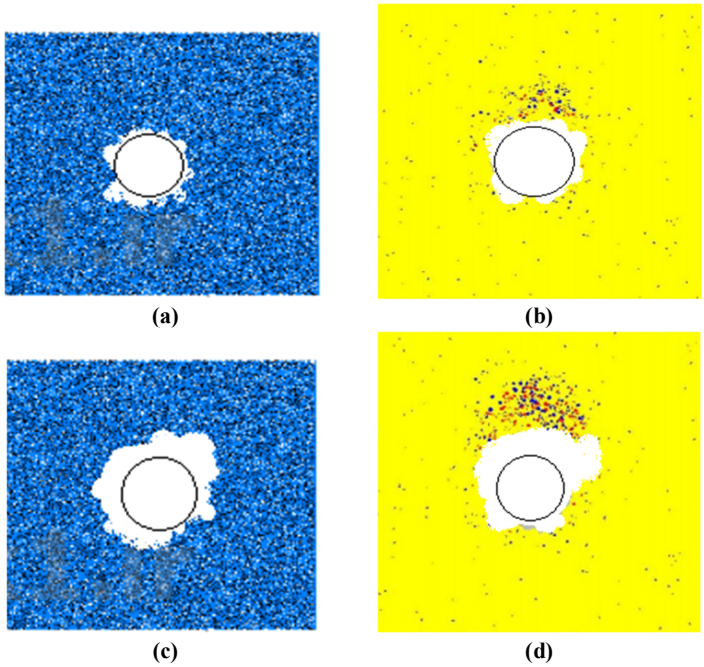

Figure 9. Comparison of simulated models with Yifie's models: a) Simulation results with fluid pressure of 10 MPa, b) Yifie's results [53] at a fluid pressure of 10 MPa, c) Simulation results at a fluid pressure of 25 MPa, d) Yifie's results [53] at a fluid pressure of 25 MPa.

5. Numerical modeling results

The modelling results of sand production without fracturing in the research [27] are the benchmark against which the new results can be compared. In the first three cases, the length of the fracture is shorter than the radius of the well. We also check to include a fracture angled different from the first (a=15 mm, r = 30 mm). The production of sand increases when a crack is created compared to the case without a crack (Figure 10a). When two cracks are placed at a 90-degree angle (Figure 10b), the production rate becomes milder and is not significantly different from the case of a 180-degree angle (Figure 10c). In general, the amount of sand production increases in this case (Figure 10d). The minimum and maximum levels of sand production are 140 gram and 450 gram, respectively.

In the second case, the fracture length equals the radius of the well. At the beginning of sandblasting, the amount of sand production is higher than in the previous state, but the overall production rate is lower (Figure 11). The minimum and maximum levels of sand production are 200 and 350 gram, respectively. The maximum amount of sand production when a < r is equal to 450 grams and when a = r is equal to 340 grams (Figure 11d).

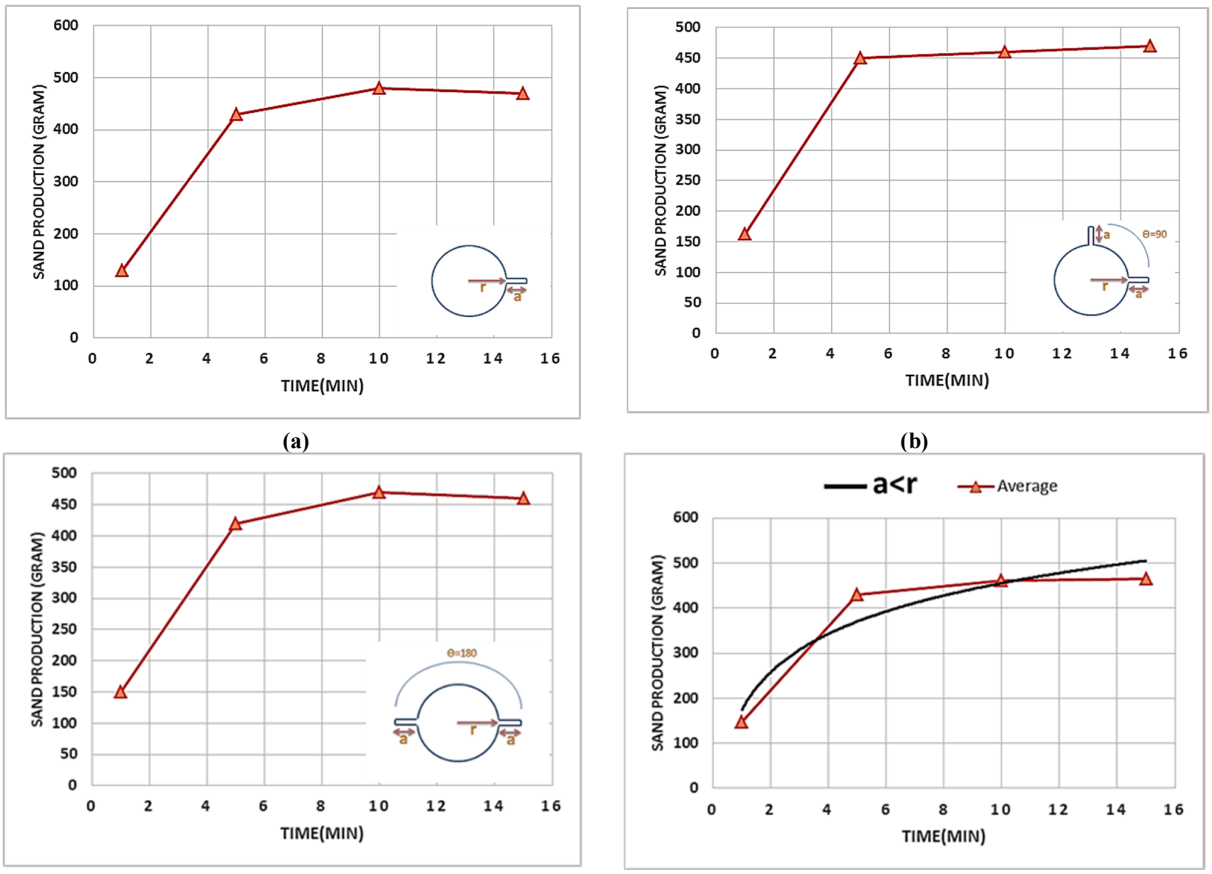

Figure 10. Modeling results for the case where the crack length is less than the radius of the well (a=15mm< r =30mm), a) One fracture, b) Two fractures with an angle of 90 degrees to each other, c) Two fractures with an angle of 180 degrees to each other, d) The average of the previous three states.

In the final scenario, where the fracture length exceeds the well radius, the likelihood of sanding initiation has decreased and the trend of the production rate is almost the same in all three cases (see Figure 12). The minimum and maximum levels of sand production are 100 and 290 gram, respectively. The maximum amount of sand production when, a > r is equal to 300 grams and when, a = r is equal to 340 grams (Figure 12). The decrease in sand production rate is noticeable compared to the previous six cases.

6. Discussion

The purpose of this section is to compare the results of hydraulic fracture modelling with sand production modelling. The research [27] explains the sand production process through laboratory tests, samples, and numerical modeling results. The models of the hydraulic fractures are similar to the models that were created in the above mentioned research. Figure 13 shows the sand production model and its results [27]. The minimum and maximum levels of sand production are 270 and 400 gram, respectively. Figure 14 shows the sand production in the modeled area after hydraulic fracturing.

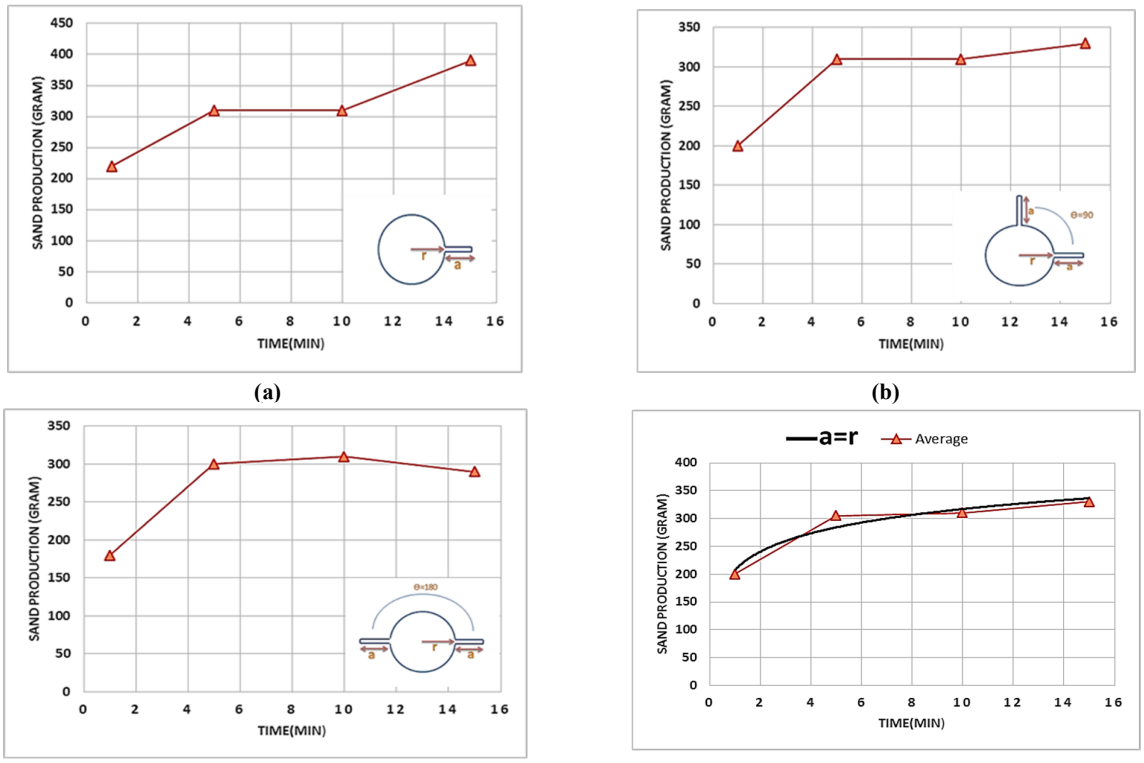

Figure 11. Modeling results for cases where the length of the crack is equal to the radius of the well (a= r =30 mm), a) One fracture, b) Two fractures with an angle of 90 degrees to each other, c) Two fractures with an angle of 180 degrees to each other, d) The average of the previous three states.

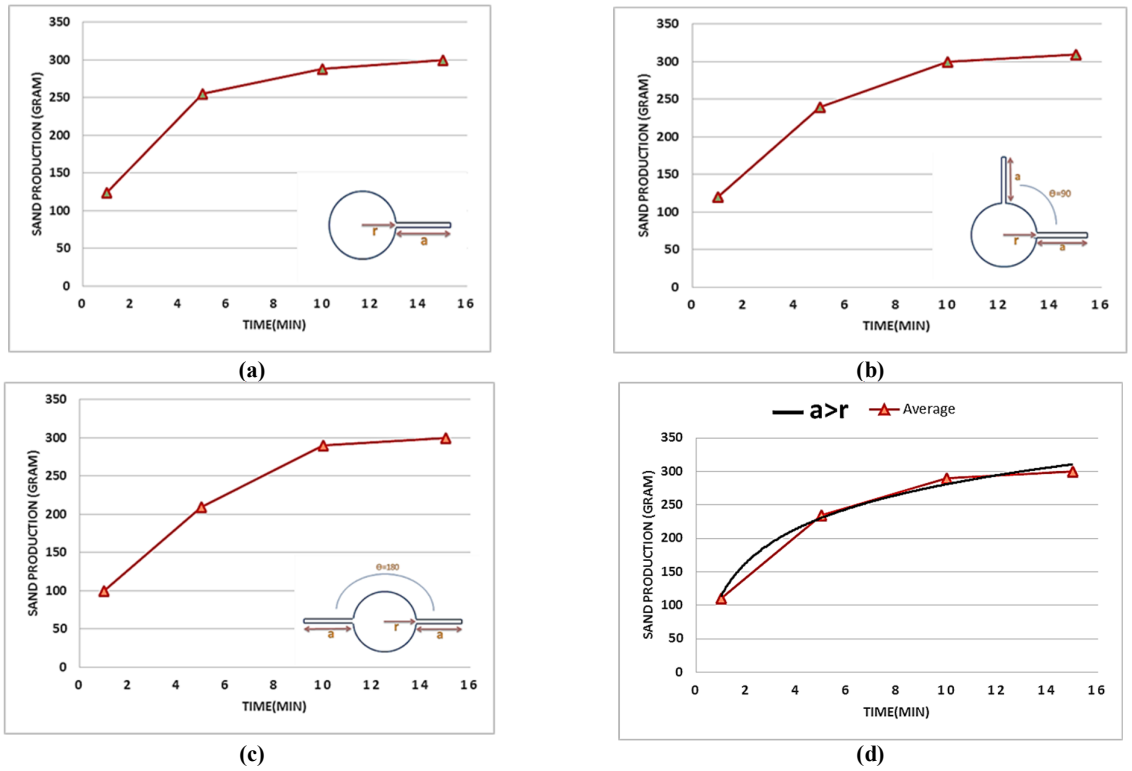

Figure 12. Modeling results for the case where the crack length is less than the radius of the well (a=50 mm> r =30 mm), a) One fracture, b) Two fractures with an angle of 90 degrees to each other, c) Two fractures with an angle of 180 degrees to each other, d) The average of the previous three states.

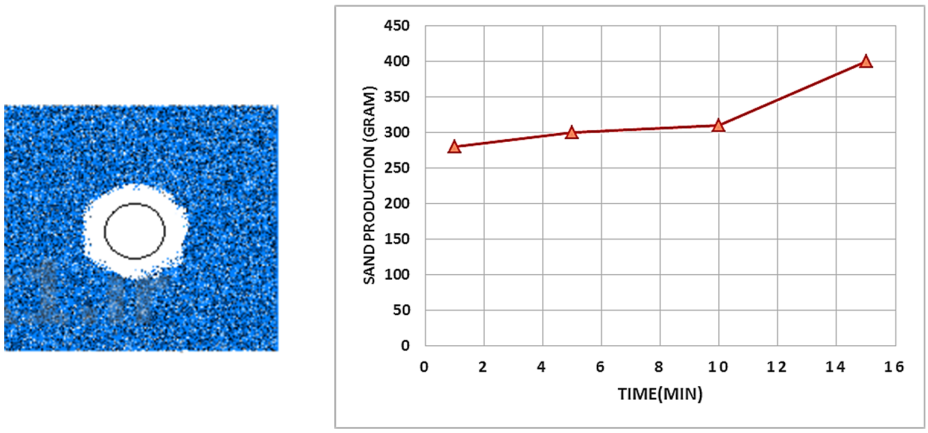

(a) (b)

Figure 13. a) Modeled section of sand production before hydraulic fracturing, b) Graph of sand production before hydraulic fracturing [27].

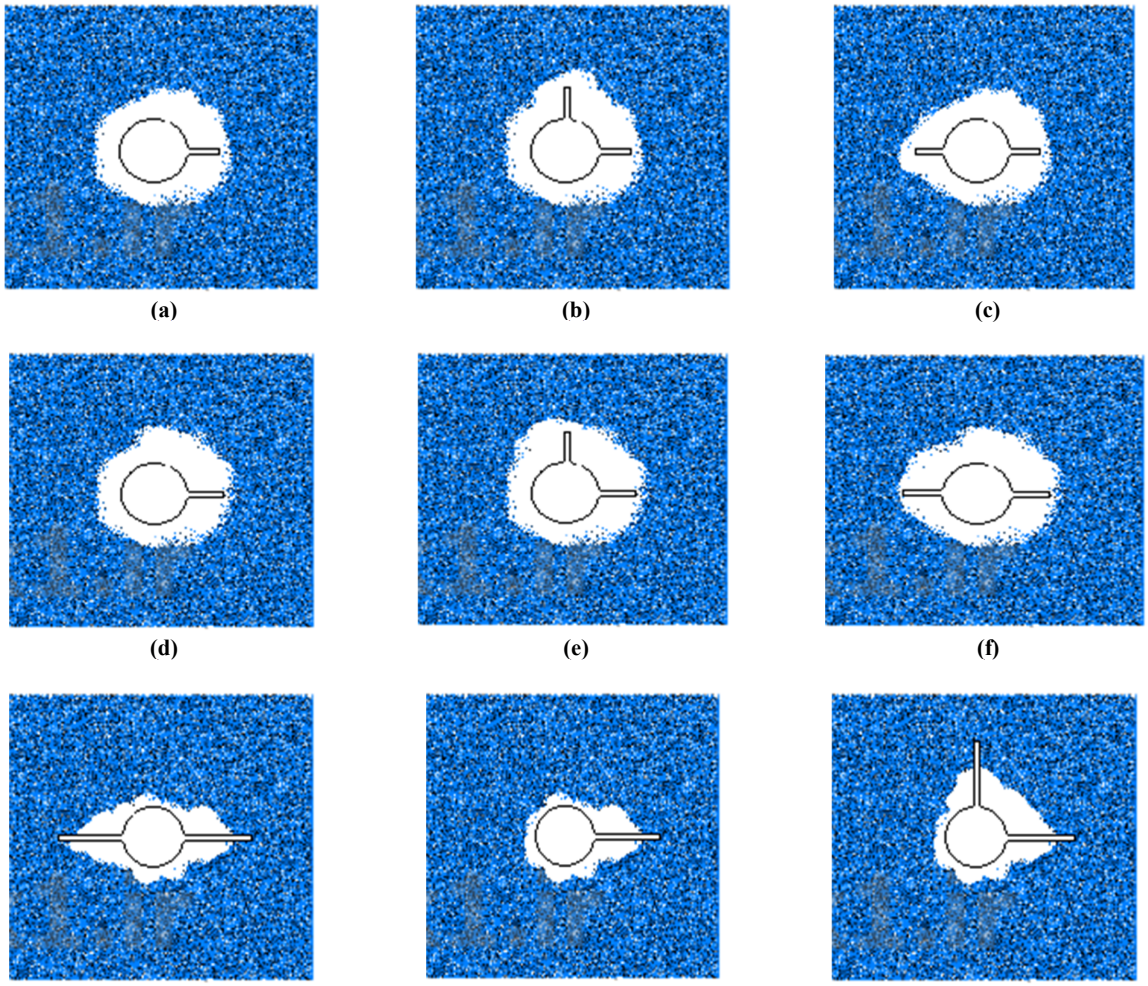

(a) (b) (c)

(d) (e) (f)

(g) (h) (i)

Figure 14. Modeled sections with 35 MPa stress and 2 MPa fluid pressure, a) One fracture (a< r), b) Two fractures with an angle of 90 degrees to each other (a< r), c) Two fractures with an angle of 180 degrees to each other (a< r), d) fracture (a= r), e) Two fractures with an angle of 90 degrees to each other (a= r), f) Two fractures with an angle of 180 degrees to each other (a= r), g) fracture (a> r), h) Two fractures with an angle of 90 degrees to each other (a>r), i)) Two fractures with an angle of 180 degrees to each other (a> r).

The sand production graph shows (Figure 15) that sand production increases significantly after hydraulic fracturing (HF). The red line of the graph shows the pre-HF sand production, which averages about 200 g/min. The blue line in the graph shows sand production after HF, which averages about 400 g/min. This shows that HF almost doubles the sand production. This increase in sand production is due to several factors. Firstly, HF causes the rock to fracture and open pores. This allows water and sand to flow more easily through the rock. Secondly, HF makes the sand finer and more granular.

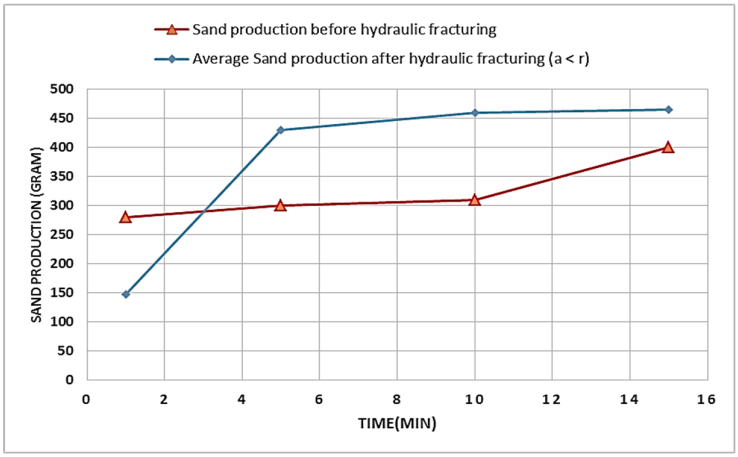

Figure 15. Sand production rate before and after hydraulic fracture - length of fracture (a) is less than the radius of the well (r).

The graph shows in Figure 16, Figure 17 the average sand production before and after hydraulic fracturing. The average sand production before hydraulic fracturing is higher than the average sand production after hydraulic fracturing. This suggests that hydraulic fracturing can be an effective way to reduce sand production.

There are a few possible explanations for this. One possibility is that hydraulic fracturing creates new pathways for the flow of oil and gas, which reduces the pressure on the formation and makes it less likely that sand will be produced. Another possibility is that the fracturing fluid helps to consolidate the formation, making it less likely that sand grains will be able to detach and flow into the wellbore. It is important to note that the effectiveness of hydraulic fracturing in reducing sand production can vary depending on the specific formation and the fracturing treatment that is used. In some cases, hydraulic fracturing can actually increase sand production. For example, if the fracturing fluid is not compatible with the formation, it can weaken the rock and make it more likely that sand will be produced.

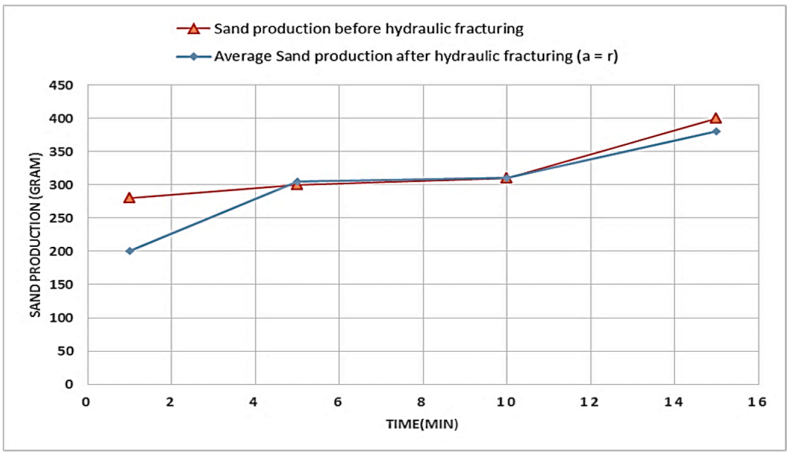

Figure 16. Sand production rate before and after hydraulic fracture - length of fracture (a) is equal to the radius of the well (r).

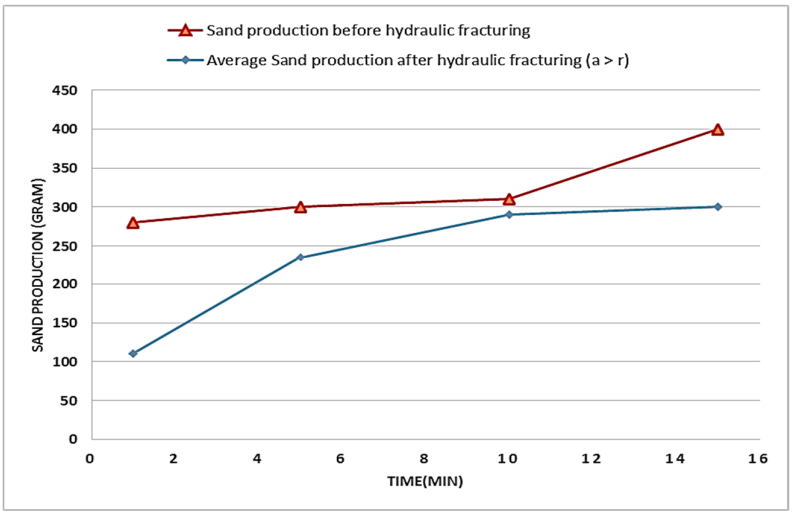

Figure 17. Sand production rate before and after hydraulic fracture - the length of the fracture (a) is greater than the radius of the well (r).

Hydraulic fracturing in oil wells can influence the mechanism of sand production, the increased pressure and stimulation from hydraulic fracturing can alter the stress distribution in the reservoir rock, potentially leading to changes in sand production patterns. Factors such as the geomechanical properties of the rock, the type and size of proppant used and the characteristics of the reservoir itself can all influence the likelihood and extent of sand production.

7. Conclusions

Sand production as one of the problems in the production stage of a wellbore was studied. A 2d discrete element model was built to study the volume of sand production in a wellbore. Fractures were incorporated into the model, resulting in a significant alteration of sand production due to changes in length and angle. Changing the angle of the fracture, except in few cases ($\theta = 180^{\circ}$), does not have much effect on changing the sand production rate. Changing the fracture length plays a greater role in changing the sand production rate. If the length of the fracture is less than the radius of the well (a < r), it can be concluded that the amount of sand production is higher than in other cases because the crack is located almost in the crushed zone. If the length of the fracture exceeds the radius of the well (a > r), the release of stresses causes a decrease in pressure, resulting in a reduction in sand production. Hydraulic fracturing can induce reservoir compaction, which refers to the settling or compression of the rock formation due to the removal of fluids. This compaction can cause sand to be released from the formation and produced along with the hydrocarbons. During the fracking process, issues such as screenouts (blockages in fractures) or formation damage can occur. These issues may result in the migration of fines and sand particles, leading to increased sand production during the well's operational life. The impact of hydraulic fracturing on sand production can vary based on reservoir-specific factors, such as the mineralogy of the formation, the geomechanical properties, and the presence of natural fractures. The average sand production before hydraulic fracturing is higher than the average sand production after hydraulic fracturing. This suggests that hydraulic fracturing can be an effective means of reducing sand production. It is important to note that the effectiveness of hydraulic fracturing in reducing sand production can vary depending on the specific formation and fracturing treatment used. In some cases, hydraulic fracturing can actually increase sand production. For example, if the fracturing fluid is not compatible with the formation, it can weaken the rock and make it more likely that sand will be produced. In summary, hydraulic fracturing can influence sand production through various mechanisms, and managing this aspect is crucial for the overall success and sustainability of unconventional oil extraction.

References

[1]. Adachi J, Siebrits E, Peirce A, Desroches J. (2007). Computer simulation of hydraulic fractures. *Int J Rock Mech Min Sci. 44(5):* 739–757.

[2]. He Q, Suorineni FT, Oh J. (2016). Review of hydraulic fracturing for preconditioning in cave mining. *Rock Mech Rock Eng. 49(12):*4893–4910.

[3]. Nadimi S, Miscovic I, McLennan J. (2016). A 3D peridynamic simulation of hydraulic fracture process in a heterogeneous medium. *J Petrol Sci Eng. 145:*444–452.

[4]. Carter BJ, Desroches J, Ingrafea AR, Wawrzynek P. (2000). Simulating fully 3D hydraulic fracturing. John Wiley and Sons, New York, pp. 525–557.

[5]. Davies RJ, Mathias SA, Moss J, and Hustoft S, Newport L. (2012). Hydraulic fractures: How far can they go? *Marine Petroleum Geol.* 37(1): 1–6.

[6]. Kim K, Rutqvist J, Nakagawa S, Birkholzer J. (2017). TOUGH-RBSN simulator for hydraulic fracture propagation within fractured media: Model validations against laboratory experiments. *Compute Geosci. 108:*72–85.

[7]. Bakhshi E, Golsanami N, Chen L. (2020). Numerical modeling and lattice method for characterizing hydraulic fracture propagation: A review of the numerical, experimental, and field studies. *Archives Compute Methods Eng.*

[8]. Hattori G, Trevelyan J, Augarde CE, Coombs WM, Aplin AC. (2016). Numerical simulation of fracking in shale rocks: current state and future approaches. *Archives Comput Methods Eng. 24(2):*281–317.

[9]. Li Q, Xing H, Liu J, Liu X. (2015). A review on hydraulic fracturing of unconventional reservoir. Petroleum. 1(1):8–15.

[10]. Zeng Q, Liu Z, Wang T, Gao Y, Zhuang Z. (2018). Fully coupled simulation of multiple hydraulic fractures to propagate simultaneously from a perforated horizontal wellbore. *Comput Mech. 61(1):*137–155.

[11]. Zhao HJ, Ma FS, Guo J. (2020). Investigation of hydraulic fracturing mechanism by using a coupled continuous-discontinuous hydromechanical model. *IOP Conf Series Earth Environ Sci. 570*:042042.

[12]. Eshiet KI, Sheng Y, Ye J. (2013). Microscopic modelling of the hydraulic fracturing process. *Environ Earth Sci. 68(4)*:1169–1186.

[13]. Wang T, Zhou W, Chen J, Xiao X, Li Y, Zhao X. (2014). Simulation of hydraulic fracturing using particle flow method and application in a coal mine. *Int J Coal Geol. 121*:1–13.

[14]. Hofmann H, Babadagli T, Yoon JS, Blöcher G, Zimmermann G. (2016). A hybrid discrete/finite element modeling study of complex hydraulic fracture development for enhanced geothermal systems (EGS) in granitic basements. *Geothermics. 64:*362–381.

[15]. Shimizu H, Murata S, Ishida T. (2011). The distinct element analysis for hydraulic fracturing in hard rock considering fluid viscosity and particle size distribution. *Int J Rock Mech Min Sci. 48(5):*712–727.

[16]. Abdollahipour A, Fatehi Marji M. (2020). A thermo-hydromechanical displacement discontinuity method to model fractures in high-pressure, high-temperature environments. *Renewable Energy*

[17]. Abdollahipour A, Fatehi Marji M, Yarahmadi Bafghi A, Gholamnejad A. (2019). complete formulation of an indirect boundary element method for poroelastic rocks. *Computers and Geotechnics.74.*15-17.

[18]. Abdollahipour A, Fatehi Marji M, Yarahmadi Bafghi A ,Gholamnejad J. (2016). Numerical investigation of effect of crack geometrical parameters on hydraulic fracturing process of hydrocarbon reservoirs. *Journal of Mining and Environment.7 (2):* 205-214

[19]. Mohammad Fatehi Marji, Lak M, Sanei M. (2023). The explosive fracturing technique analysis for highly low permeable reservoirs using analytical, displacement discontinuity and finite difference coupled method.

[20]. Dusseault MB, Santarelli FJ A. (1989). Conceptual model for massive solids production in poorly-consolidated sandstones. *Rock at great depth. 2(1):* 789–797.

[21]. Fjaer E, Holt RM, Horsrud P, Raaen AM, Risnes R. (1992). *Petroleum related rock mechanics*. Amsterdam.

[22]. A. Hauwa Christiana, A. (2015). Sand control using geomechanical techniques: A case study of Niger delta, Nigeria, *Journal of science inventions today. 5(1)*439-450.

[23]. Bianco LC. (1999). Phenomena of sand production in non-consolidated sandstones, PhD thesis. Penn State University, University Park Penn.

[24]. Sanei M, Durán O, Devloo PRB, Santos ESR. (2021). Analysis of pore collapse and shear-enhanced compaction in hydrocarbon reservoirs using coupled poro elastoplasticity and permeability. *Arab J Geosci. 14(7).*

[25]. Abdollahipour A, Kargar A, Fatehi Marji M. (2023). Numerical modeling of the effect of Anderson's stress regimes on the volume of sand production in oil wellbores. *Journal of Analytical and Numerical Methods in Mining Engineering. 13(35):* 31-38.

[26]. Abdollahipour A, Fatehi Marji M. (2023). Numerical modeling of borehole breakouts formation in various stress fields using a Higher-Order Displacement Discontinuity Method (HODDM). *Journal of Petroleum Geomechanics. 4(3):* 1-18.

[27]. Yazdani M, Fatehi Marji M, Najafi M, Sanei M. (2023). Discrete elements analysis of sand production mechanism in oil well considering effects of in situ

stress and fluid pressure. *Journal of Mining and Environment.*

[28]. Lecampion B, Bunger A, Zhang X. (2018). Numerical methods for hydraulic fracture propagation: a review of recent trends. *J Nat Gas Sci Eng. 49*:66–83.

[29]. Chen B, Barron AR, Owen D, Li C. (2018). Propagation of a plane strain hydraulic fracture with a fluid lag in permeable rock. *J Appl Mech. 85(9):*091003–091010.

[30]. Garagash DI, Detournay E. (2005). Plane-strain propagation of a fluid-driven fracture: small toughness solution. *J Appl Mech. 72(6):*916–928.

[31]. Lecampion B. (2009). An extended finite element method for hydraulic fracture problems. *Commun Numer Methods Eng. 25(2):*121–133.

[32]. Biot MA. (1941). General theory of three-dimensional consolidation. *J Appl Phys.12 (2):*155–164.

[33]. Gupta P, Duarte CA. (2014). Simulation of non-planar three-dimensional hydraulic fracture propagation. *Int J Numer Anal Methods Geomech. 38(13):*1397–1430.

[34]. Deb P, Salimzadeh S, Vogler D, Dueber S, Clauser C, Settgast RR. (2021). Verifcation of coupled hydraulic fracturing simulators using laboratory-scale experiments. *Rock Mech Rock Eng.*

[35]. Zhang X, Jefrey RG, Thiercelin M. (2009). Mechanics of fluid-driven fracture growth in naturally fractured reservoirs with simple network geometries. *Journal of Geophysical Research. 114*(B12).

[36]. Paluszny A, Thomas RN, Saceanu MC, Zimmerman RW. (2020). Hydro-mechanical interaction effects and channeling in three dimensional fracture networks undergoing growth and nucleation. *J Rock Mech Geomech Eng. 12(4):*707719.

[37]. Secchi S, Schrefer BA. (2012). A method for 3-d hydraulic fracturing simulation. *Int J Fracture. 178(1–2):* 245–258.

[38]. Lecampion B, Bunger A, Zhang X. (2018). Numerical methods for hydraulic fracture propagation: a review of recent trends. *J Nat Gas Sci Eng. 49*:66–83.

[39]. Zia H, Lecampion B. (2020). Pyfrac: A planar 3D hydraulic fracture simulator. *Comput Phys Commun. 255:*107368.

[40]. Sarris E, Papanastasiou P. (2011). The influence of the cohesive process zone in hydraulic fracturing modelling. *Int J Fracture. 167(1):*33–45.

[41]. Rahman MK, Hossain MM, Rahman SS. (2000). An analytical method for mixed-mode propagation of pressurized fractures in remotely compressed rocks. *Int J Fracture. 103(3):*243–258.

[42]. Dugdale DS. (1960). Yielding of steel sheets containing slits. *J Mech Phys Solids. 8(2):*100–104.

[43]. Barenblatt GI. (1962). the mathematical theory of equilibrium cracks in brittle fracture. 7:55–129.

[44]. Li LC, Tang CA, Li G, Wang SY, Liang ZZ, Zhang YB. (2012). Numerical simulation of 3D hydraulic fracturing based on an improved flow-stress-damage model and a parallel fem technique. *Rock Mech Rock Eng.*

[45]. Yuonessi A, V. B. (2013). Sand production simulation under true-triaxial stress conditions. *International Journal of Rock Mechanics and mining Science.61*: 130-140.

[46]. Fjaer .E, Holt RM, Horsrud P, Raaen AM, Risnes R. (1992). Petroleum related rock mechanics. Amsterdam.

[47]. Cundall P. (1971). A computer model for simulating progressive large scale movements in blocky rock systems. *In: Symposium of International Society of Rock Mechanics*, II-8

[48]. Wang T, Zhou W, Chen J, Xiao X, Li Y, Zhao X. (2014). Simulation of hydraulic fracturing using particle flow method and application in a coal mine. *Int J Coal Geol. 121*:1–13.

[49]. Al-Busaidi A, Hazzard JF, Young RP. (2005). Distinct element modeling of hydraulically fractured lac du bonnet granite. *J Geophysics Res.*

[50]. Wang T, Liu Z, GAO Y, Zeng Q, Zhuang Z. (2017). Theoretical and numerical models to predict fracking debonding zone and optimize perforation cluster spacing in layered shale. *J Appl Mech .85(1):*011001.

[51]. Qu T, Feng Y, Wang M, Jiang S. (2020). Calibration of parallel bond parameters in bonded particle models via physics-informed adaptive moment optimisation. *Powder Techno. 366*: 527–536.

[52]. Rahmati H, A. N. (2011). Validation of predicted cumulative sand and sand rate against physical-model test. *Journal of Canadian Petroleum Technology. 51(5):* 403–410.

[53]. C. yufi, A. E. (2016). A new approach to dem simulation of sand production. *Journal of Petroleum Science and Engineering. 147*: 56-67.

[54]. Natalia Climent Pera. (2016). A Coupled CFD-DEM Model for Sand Production in Oil Wells. *Ph.D. thesis,* Barcelona, September 2016.

شبیه سازی مکانیزم شکست هیدرولیکی در اطراف چاه های هیدروکربنی با اثرات آن بر تولید ماسه

مسعود یزدانی، محمد فاتحی مرجی*، مهدی نجفی و منوچهر صانعی

گروه مهندسی معدن و متالورژی، دانشگاه یزد، یزد، ایران

ارسال ۲۰۲۴/۰۱/۱۰، پذیرش ۲۰۲۴/۰۵/۱۳

* نویسنده مسئول مکاتبات: mohammad.fatehi@gmail.com

چکیده:

حدود ۷۰ درصد از میدان های هیدروکربنی جهان در مخازن حاوی سنگ های کم استحکام مانند ماسه سنگ واقع شده است. در طول تولید هیدروکربن ها از مخازن ماسه سنگ، ذرات به اندازه ماسه ممکن است از سازند خارج شده و وارد جریان سیال هیدروکربنی شوند. تولید شن و ماسه به دلیل پتانسیل ایجاد فرسایش لوله‌ها و شیرها، موضوع مهمی در صنعت نفت است. جداسازی دانه ها از نفت فرآیندی پرهزینه است. انگیزه شرکت های نفت و گاز کاهش تولید شن و ماسه در طول استخراج نفت است. شکست هیدرولیک یکی از پارامترهایی است که می تواند بر تولید شن و ماسه تأثیر بگذارد. با این حال، درک فعل و انفعالات پیچیده بین مکانیسم‌های شکست هیدرولیکی و تولید شن و ماسه در اطراف چاه‌ها برای بهینه‌سازی بازیابی مخزن و اطمینان از یکپارچگی چاه‌های تولیدی حیاتی است. این مقاله به بررسی رویکرد شبیه‌سازی یکپارچه برای مدل‌سازی فرآیندهای شکست هیدرولیکی و ارزیابی اثرات آن‌ها بر تولید شن و ماسه می‌پردازد. مدل های دو بعدی با استفاده از روش المان گسسته در نرم افزار PFC2D برای این تحقیق ایجاد شد. طول شکستگی در مدل ها بر اساس شعاع چاه متفاوت است. زاویه بین دو شکستگی در ۹۰ و ۱۸۰ درجه نسبت به یکدیگر نیز مدل‌سازی شد. در حالت اول طول شکستگی کمتر از شعاع چاه است، در حالت دوم مقادیر برابر است و در نهایت طول شکست بیش از شعاع چاه فرض می شود. نتایج کالیبره شده و تایید شده تغییر در نرخ تولید شن و ماسه را در مقایسه با حالت شکسته نشان می دهد.

کلمات کلیدی: روش المان مجزا؛ شکست هیدرولیکی؛ تولید ماسه؛ چاه نفت.